

## Electronic Supplementary Information

### Experimental Section

#### **Materials**

Potassium oxalate monohydrate ( $K_2C_2O_4 \cdot H_2O$ ), hydrazine monohydrate ( $N_2H_4 \cdot H_2O$ ), ammonium sulfate ( $(NH_4)_2SO_4$ ),  $^{15}N$  isotope labeled ammonium sulfate ( $^{15}NH_4)_2SO_4$ , cobalt chloride ( $CoCl_2 \cdot 6H_2O$ ), sodium molybdate ( $Na_2MO_4 \cdot 2H_2O$ ), sodium citrate ( $Na_3C_6H_5O_7 \cdot 2H_2O$ ), salicylic acid ( $C_7H_6O_3$ ), sodium nitroferricyanide dihydrate ( $C_5FeN_6Na_2O \cdot 2H_2O$ ), sodium hypochlorite ( $NaClO$ ), para(dimethylamino) benzaldehyde (p- $C_9H_{11}NO$ ), and commercial chitosan ( $C_{6n}H_{11n}NO_{4n}$ ) were bought from Aladdin Chemical Reagent Co., Ltd. Calcium carbonate nanoparticles ( $CaCO_3$ , ~67 nm) were purchased from Nanjing XFNANO Materials Tech Co., Ltd. and used as received. Chloride acid (HCl) and sodium hydroxide (NaOH) were supplied by Sinopharm Chemical Reagent Co. Ltd. Commercial carbon cloth (HCP331N) was used as substrate obtained from Shanghai Hesen electric co., Ltd. The deionized water (18.2 M $\Omega$ ) was used throughout all experiments.

#### **Preparation of N-doped porous carbon (NPC@500)**

In a typical synthesis, 1 g commercial chitosan was dissolved into 50 mL of deionized water with water bath at 80 °C under constant stirring until the full water evaporates. Then, the chitosan thoroughly mixed in a mortar with  $K_2C_2O_4 \cdot H_2O$  and  $CaCO_3$  at a weight ratio of 1:1:1. After that, the mixture was transferred into a corundum boat and heated to 500 °C for 2 h with a heating rate of 5 °C min<sup>-1</sup> in Ar atmosphere in a tube furnace. Afterward, the powder was washed with diluted HCl for several times to remove the generated inorganic impurities. Finally, the black powder was collected by filtering and repeated washing with deionized water and ethylene glycol, and then vacuum-dried at 60 °C for 24 h to obtain N-doped porous carbon. The obtained samples were denoted as NPC@500.

#### **Preparation of Co-N<sub>x</sub>/NPC@500**

The Co-N<sub>x</sub>/NPC@500 was prepared through the same procedure with the addition of 10 mL 2mg/mL cobalt chloride as Co source in the process of water bath.

#### **Preparation of Mo-N<sub>x</sub>/NPC@500**

The Mo-N<sub>x</sub>/NPC@500 was synthesized through the same procedure with the addition of 10mL 2mg/mL sodium molybdate as Mo source in the process of water bath.

### **Characterizations**

Scanning electron microscopy (SEM) images of the samples were collected on a field emission scanning electron microscope (SU 8020). Transmission electron microscopy (TEM) images of the samples were obtained on a JEOL-2010 microscope. Furthermore, the HAADF-STEM and EDX mapping experiments were performed on FEI Titan G2 microscope equipped with a Super-X detector at 300 kV. X-ray diffraction (XRD, Philips X'pert PRO) patterns were obtained by using Ni-filtered monochromatic Cu K $\alpha$  radiation ( $\lambda$  K $\alpha$ 1=1.5418 Å) at 40 kV and 40 mA. Raman spectra of the samples were collected on a Renishaw Micro-Raman Spectroscopy (Renishaw inVia Reflex) using 532 nm laser excitation. X-ray photoelectron spectroscopy (XPS) of the samples was performed on an ESCALAB 250 X-ray photoelectron spectrometer (Thermo, America) equipped with Al K $\alpha$ 1, 2 monochromatized radiations at 1486.6 eV X-ray source. Nitrogen adsorption-desorption isotherms were measured on an automated gas sorption analyzer (Autosorb-iQ-Cx). The Co and Mo content on N-doped porous carbon NPC@500 was determined by ICP-AES (ICP-6300, Thermo Fisher Scientific). The UV-vis absorbance spectra were measured on an UV-vis 2700 spectrophotometer.

### **Electrochemical Measurements**

The electrocatalytic NRR performance of the as-prepared catalysts was evaluated under ambient conditions in 0.1 M Na<sub>2</sub>SO<sub>4</sub> electrolyte using a gas-tight two-compartment cell on an electrochemical workstation (CHI 660E) in the three-electrode system. The as-prepared catalysts coated commercial carbon cloth was used as the working electrode, and Ag/AgCl (saturated KCl solution) and platinum net were used as the reference electrode and counter electrode, respectively. The working electrode was prepared as follows: 10 mg catalyst was first dispersed in 950  $\mu$ L of absolute ethanol and 50  $\mu$ L of Nafion solution (5.0 wt%) by 30 min sonication to form a homogeneous catalyst ink. After that, 10  $\mu$ L catalyst ink was loaded onto a carbon cloth (CC) with an area of 1.0  $\times$  1.0 cm<sup>2</sup> and dried under ambient conditions for further use. The catalyst loading amount was 0.1 mg cm<sup>-2</sup>. All the potentials in this work were converted to the RHE through the following equation:  $E$  (V vs RHE) =  $E$  (V vs Ag/AgCl) + 0.197 + 0.059  $\times$  pH. Linear sweep voltammetry (LSV) measurements of the catalysts were conducted in Ar- and N<sub>2</sub>-saturated 0.1 M Na<sub>2</sub>SO<sub>4</sub> solution with a scan rate of 10 mV s<sup>-1</sup>.

### **Isotope Labeling Experiments**

The <sup>14</sup>N and <sup>15</sup>N isotopic labeling experiments were conducted using <sup>14</sup>N<sub>2</sub> and <sup>15</sup>N<sub>2</sub> as the feeding gases (99% enrichment of <sup>15</sup>N in <sup>15</sup>N<sub>2</sub>, supplied by Hefei Ninte Gas Management Co., Ltd.). Prior to use for NRR measurements, <sup>14</sup>N<sub>2</sub> and <sup>15</sup>N<sub>2</sub> feeding gases were go through purification system (Fig. S3). After the electrochemical reaction in 0.1 M Na<sub>2</sub>SO<sub>4</sub> solution at -0.4 V (vs RHE) for 1 h, 1 mL 0.5 M H<sub>2</sub>SO<sub>4</sub> were added to acidify the electrolyte. Then, the solution was concentrated to 1.0 mL at 80 °C. Then, 0.8 mL of above solution mixed with 0.2 mL of D<sub>2</sub>O was used for <sup>1</sup>H NMR spectroscopy measurement (Bruker AVANCE AV III 400). The <sup>1</sup>H NMR analysis were carried out in accordance with the reported method.<sup>1,2</sup>

### **Determination of NH<sub>3</sub>**

After the NRR measurement, the formed NH<sub>3</sub> product was detected by the indophenol blue method. In detail, 10 mL of electrolyte taken from the cathodic chamber and mixed with 500 μL of 1.0 M NaOH solution containing 5.0 wt% sodium citrate and 5.0 wt% salicylic. 100 μL of 1.0 wt% sodium nitroferricyanide solution and 100 μL of 0.55 M NaClO solution were added to the sample solution, sequentially. After maintaining for 1 h at room temperature, the UV–vis absorption spectrum was measured at a wavelength of 700 nm. The concentration (NH<sub>4</sub><sup>+</sup>-N) absorbance curves were calibrated using standard ((NH<sub>4</sub>)<sub>2</sub>SO<sub>4</sub>) solution with NH<sub>4</sub><sup>+</sup>-N concentrations of 0.0, 0.05, 0.1, 0.2, 0.4, 0.6, 0.8, and 1.0 μg mL<sup>-1</sup> in 0.1 M Na<sub>2</sub>SO<sub>4</sub>. The fitting curve ( $y = 1.034x - 0.009$ ,  $R^2 = 0.999$ ) showed good linear relation of the NH<sub>4</sub><sup>+</sup>-N concentration with absorbance value.

### **Determination of N<sub>2</sub>H<sub>4</sub>**

The Watt and Chrisp method was applied to estimate the possible produced N<sub>2</sub>H<sub>4</sub> during the NRR. The p-C<sub>9</sub>H<sub>11</sub>NO (5.99 g), HCl (30 mL), and C<sub>2</sub>H<sub>5</sub>OH (300 mL) were first mixed as a color reagent. Typically, 1.0 mL of electrolyte was removed from the electrochemical reaction chamber, was acidized with 9.0 mL of 1.0 M HCl solution, and then added into 5.0 mL of color reagent with rapid stirring for several times at room temperature. After 20 min, the mixture was measured on an UV–vis 2700 spectrophotometer at a wavelength of 455 nm. The obtained calibration curve was used to calculate the hydrazine concentration. And the fitting curve showed a good linear relation of absorbance with the N<sub>2</sub>H<sub>4</sub>·H<sub>2</sub>O concentration ( $y = 1.74x + 0.0108$ ,  $R^2 = 0.999$ ).

The NH<sub>3</sub> yield rate (R) was calculated by the following equation:

$$R_{\text{NH}_3} = (\text{NH}_4^+\text{-N}) \times 17 \times V / (14 \times t \times m_{\text{cat.}}) \quad (1)$$

FE was calculated according to following equation:

$$\text{FE} = 3 \times F \times (\text{NH}_4^+\text{-N}) \times V / (14 \times Q) \quad (2)$$

Where (NH<sub>4</sub><sup>+</sup>-N) is the measured (NH<sub>4</sub><sup>+</sup>-N) concentration; V is the total volume of the cathodic reaction electrolyte; t is reaction time; m<sub>cat.</sub> is the loading quality of catalyst; F is the Faraday constant and Q is the total charge during the reaction process according to the corresponding current density.

Table S1. Elemental composition of the NPC@500 by XPS technique.

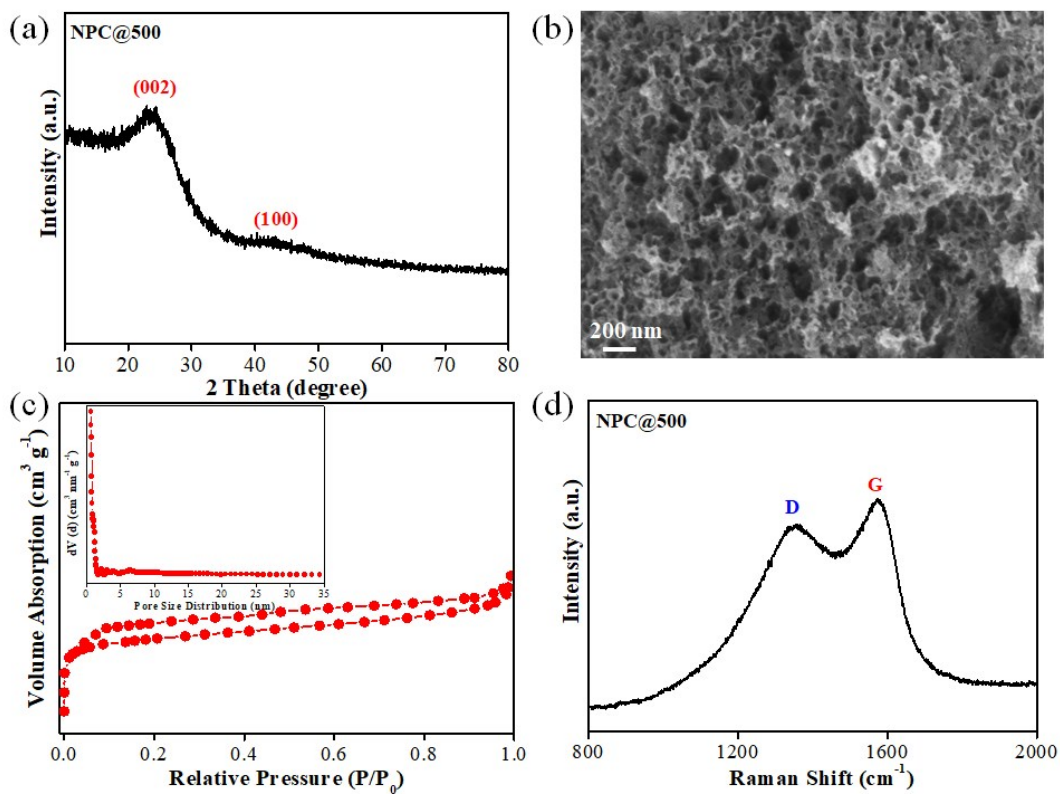
Sample	N (at%)	pyrrolic-N	pyridinic-N	pyrrolic-N/N	pyridinic-N/N	C (at%)	O (at%)
NPC@500	7.15	66.78	33.22	4.77	2.37	78.52	14.60
NPC@500-Ar	5.81	62.45	37.54	3.63	2.18	77.92	16.27

Table S2. Elemental composition of the NPC@500 and Co-N<sub>x</sub>/NPC@500 by elemental analyser test.

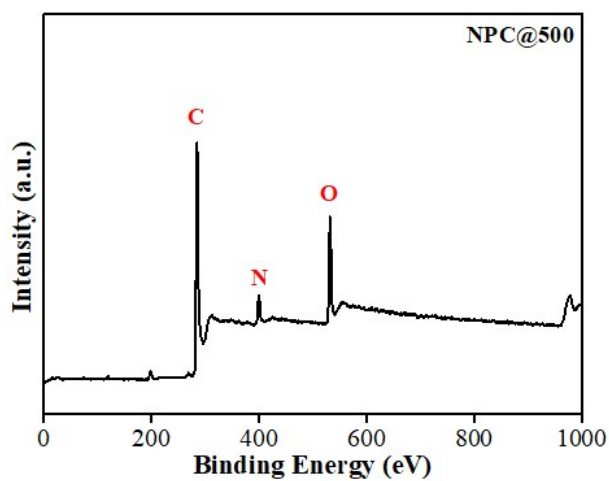
Sample	N(%)	C(%)	H(%)
NPC@500	9.45	66.99	2.339
NPC@500-Ar	7.67	61.81	2.765
Co-N <sub>x</sub> /NPC@500	8.36	60.74	2.935
Co-N <sub>x</sub> /NPC@500-N <sub>2</sub>	8.41	61.01	2.875

Table S3. Elemental composition of the Co or Mo-N<sub>x</sub>/NPC@500 by XPS technique.

Sample	N (at.%)			N (at%)	C (at%)	O (at%)	Co (at%)	Mo (at%)
	pyrrolic-N	pyridinic-N	Co-N or Mo-N					
Co-N <sub>x</sub> /NPC@500	20.81	29.42	49.76	7.20	78.42	13.85	0.53	/
Co-N <sub>x</sub> /NPC@500-N <sub>2</sub>	20.49	30.02	49.49	7.15	77.17	15.17	0.51	/
Mo-N <sub>x</sub> /NPC@500	76.95	20.33	2.72	7.11	78.85	13.82	/	0.22
Mo-N <sub>x</sub> /NPC@500-N <sub>2</sub>	77.08	20.22	2.70	7.08	77.52	15.15	/	0.25



**Fig. S1.** (a) XRD pattern, (b) SEM image, (c) N<sub>2</sub> adsorption–desorption isotherms, and (d) Raman spectra of NPC@500.



**Fig. S2.** XPS spectra of NPC@500.

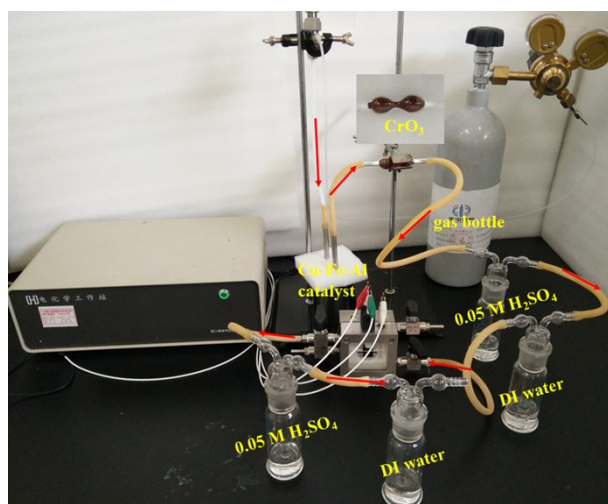


**Fig. S3.** Optical photograph of the NRR measurement system including two-compartment electrochemical cell with three-electrode configuration and two-series tail gas absorbers.

In order to achieve accurate experimental results and eliminate the interferences of possible contamination from environment of the  $\text{NH}_3$  synthesis. All measurements experimental system possess  $\text{N}_2$  (or Ar) feeding gas purification system and tail gas  $\text{NH}_3$  recovery system. To remove  $\text{NO}_x$ , a Cu impurity trap unit was introduced, composed of Cu-Fe-Al catalyst in a U shaped stainless steel tubing. Furthermore, a  $\text{CrO}_3$  column was incorporated into the gas purification system to convert any possible NO to soluble  $\text{NO}_2$ , which can be removed by the  $\text{H}_2\text{SO}_4$  and deionized water absorption units before reaching the electrochemical cell. After NRR, the produced tail gas was further absorbed by two-series tail gas absorbers (absorber contains 20 mL of 0.05 M  $\text{H}_2\text{SO}_4$  solution and 20 mL of deionized water, respectively.) to prevent the produced  $\text{NH}_3$  flowing into air during NRR.<sup>2,3</sup>

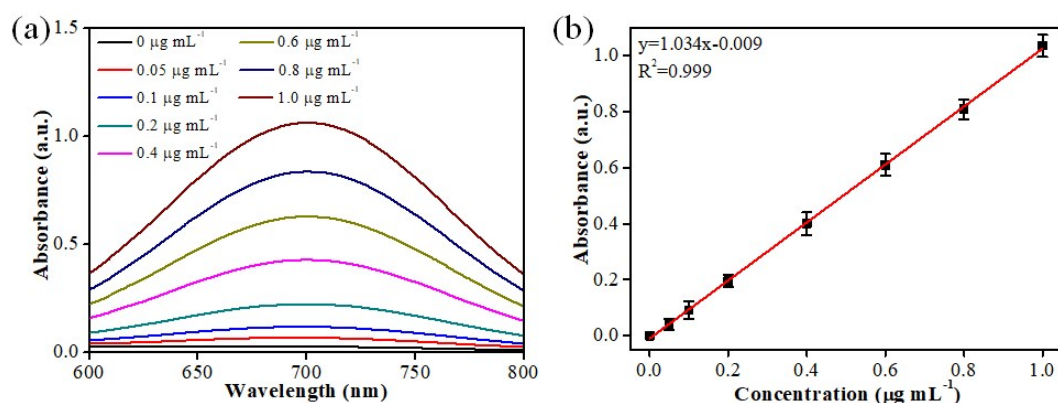


**Fig. S4.** (a) UV-vis absorption spectra of various  $\text{NH}_4^+\text{-N}$  concentrations after incubated for 1 h at room temperature. (b) Calibration curve used for calculation of  $\text{NH}_4^+\text{-N}$  concentrations.

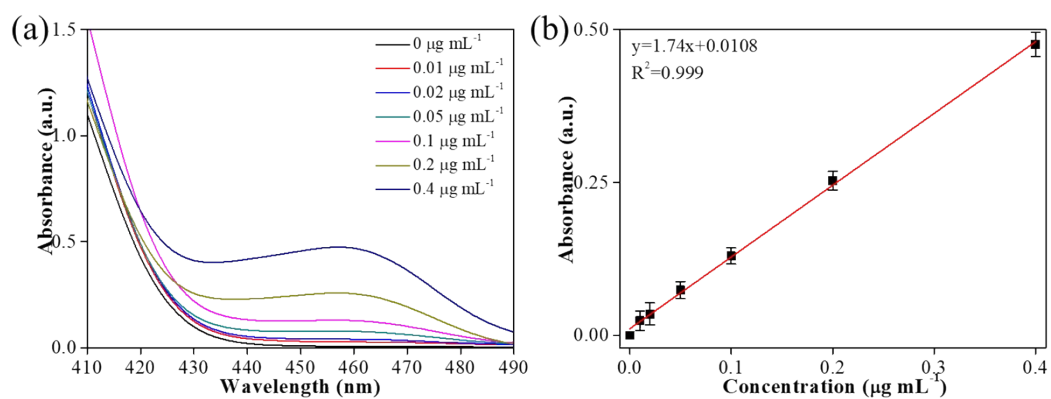


**Fig. S5.** (a) UV-vis absorption spectra of various  $\text{N}_2\text{H}_4$  concentrations after incubated for 20 min at room temperature. (b) Calibration curve used for calculation of  $\text{N}_2\text{H}_4$  concentrations.

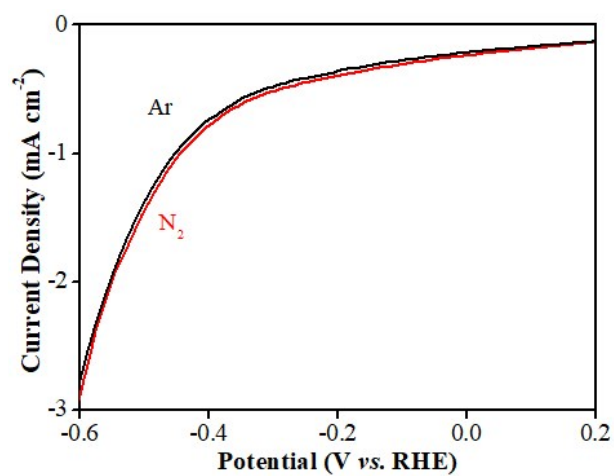


**Fig. S6.** (a) LSV curves of NPC@500 in  $\text{N}_2$ - and Ar-saturated 0.1 M  $\text{Na}_2\text{SO}_4$  electrolyte.

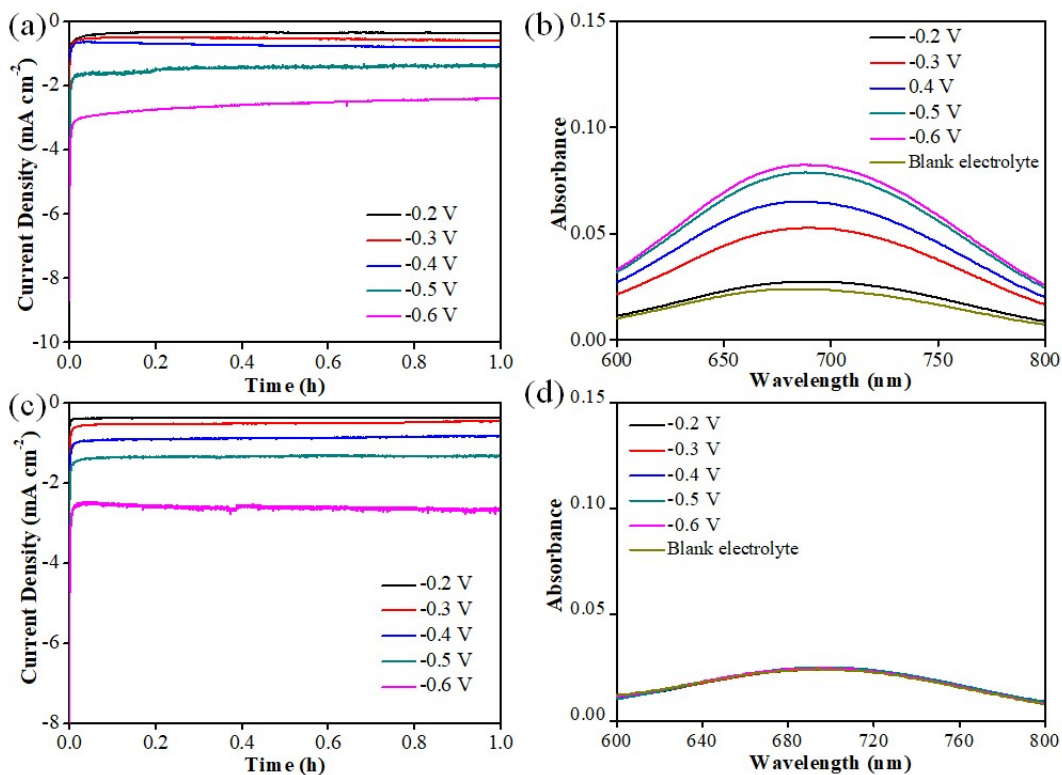


**Fig. S7.** (a) Time-dependent current density curves at various potentials in Ar-saturated 0.1 M Na<sub>2</sub>SO<sub>4</sub>. (b) UV-vis absorption spectra of the Ar-saturated 0.1 M Na<sub>2</sub>SO<sub>4</sub> electrolytes stained with indophenol indicator after 1 h electrolysis at different potentials. (c) Time-dependent current density curves at various potentials in N<sub>2</sub>-saturated 0.1 M Na<sub>2</sub>SO<sub>4</sub>. (d) UV-vis absorption spectra of the N<sub>2</sub>-saturated 0.1 M Na<sub>2</sub>SO<sub>4</sub> electrolytes stained with indophenol indicator after 1 h electrolysis at different potentials.



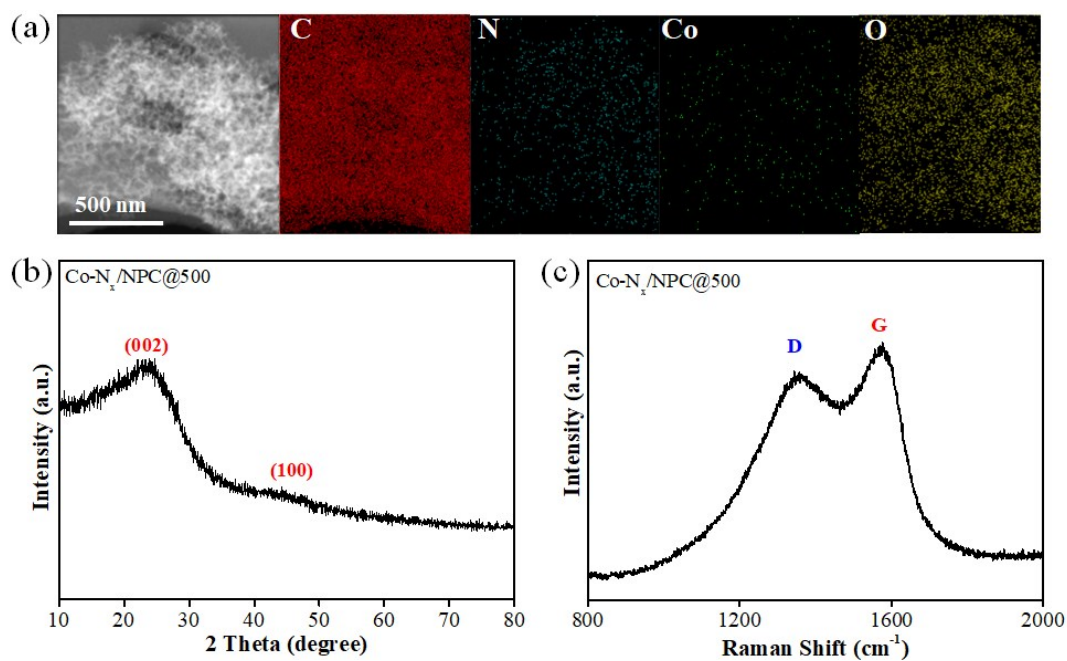


**Fig. S8.** (a) EDS images of Co-N<sub>x</sub>/NPC@500, (b) XRD pattern of Co-N<sub>x</sub>/NPC@500. (c) Raman spectra of Co-N<sub>x</sub>/NPC@500.

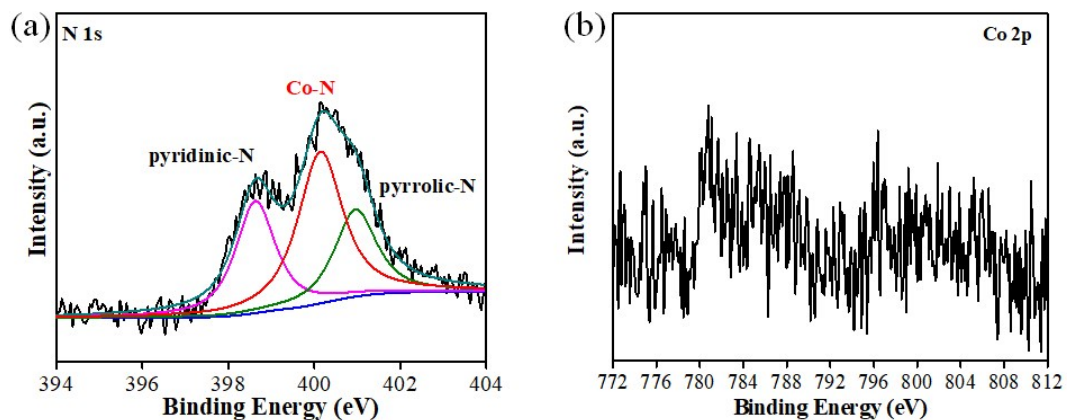


**Fig. S9.** (a) The high-resolution N 1s XPS spectra and (b) the high-resolution Co 2p XPS spectra of Co-N<sub>x</sub>/NPC@500.

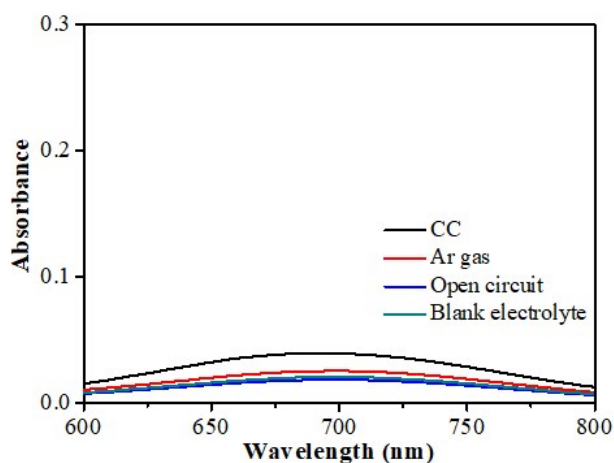


**Fig. S10.** UV-vis absorption spectrum of control experiments.

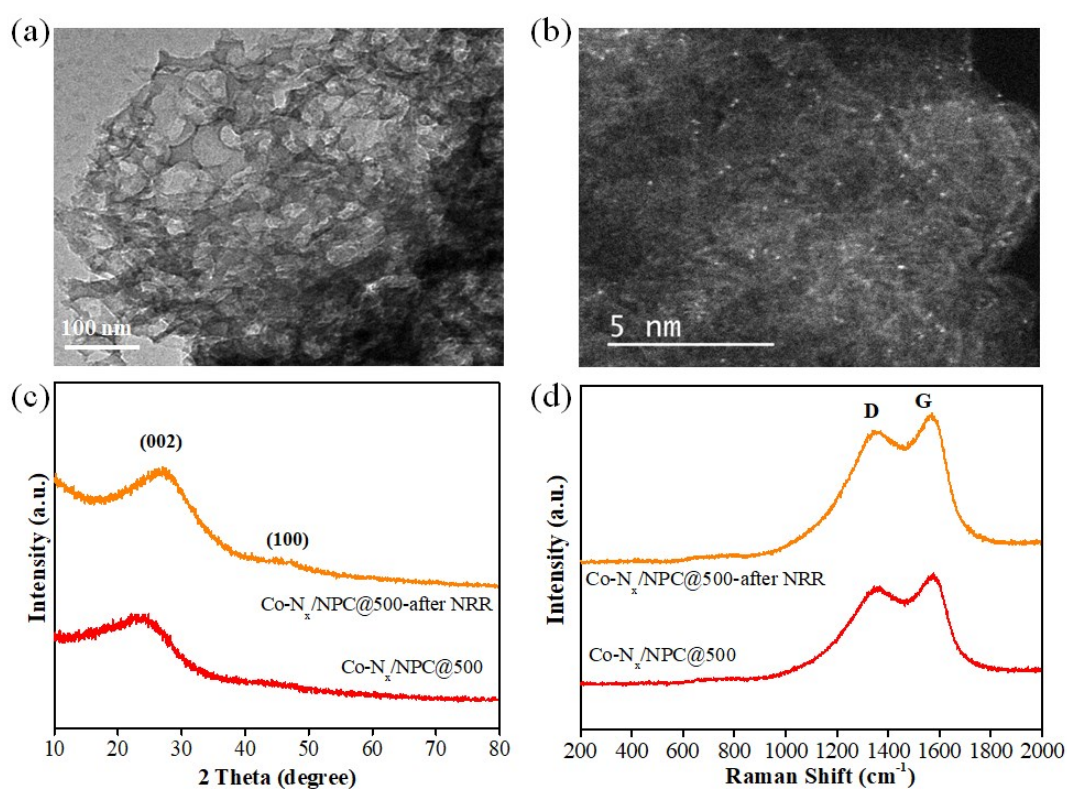


**Fig. S11.** (a) TEM image and (b) aberration-corrected HAADF-STEM image of Co-N<sub>x</sub>/NPC@500 after long-term electrocatalysis at  $-0.4$  V (vs.RHE) in N<sub>2</sub>-saturated 0.1 M Na<sub>2</sub>SO<sub>4</sub> electrolyte. (c) XRD patterns and (d) Raman spectra of Co-N<sub>x</sub>/NPC@500 before and after long-term electrocatalysis at  $-0.4$  V (vs.RHE) in N<sub>2</sub>-saturated 0.1 M Na<sub>2</sub>SO<sub>4</sub> electrolyte.

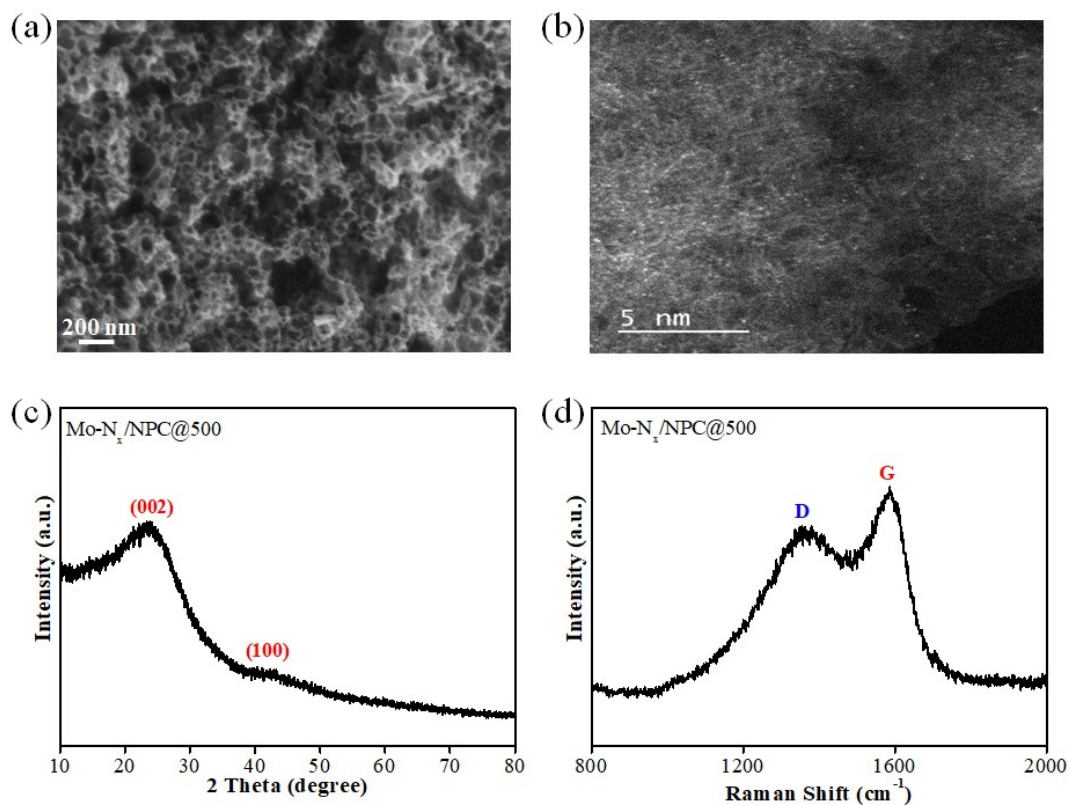


**Fig. S12.** (a) SEM image, (b) aberration-corrected HAADF-STEM image, (c) XRD pattern and (d) Raman spectra of Mo-N<sub>x</sub>/NPC@500.

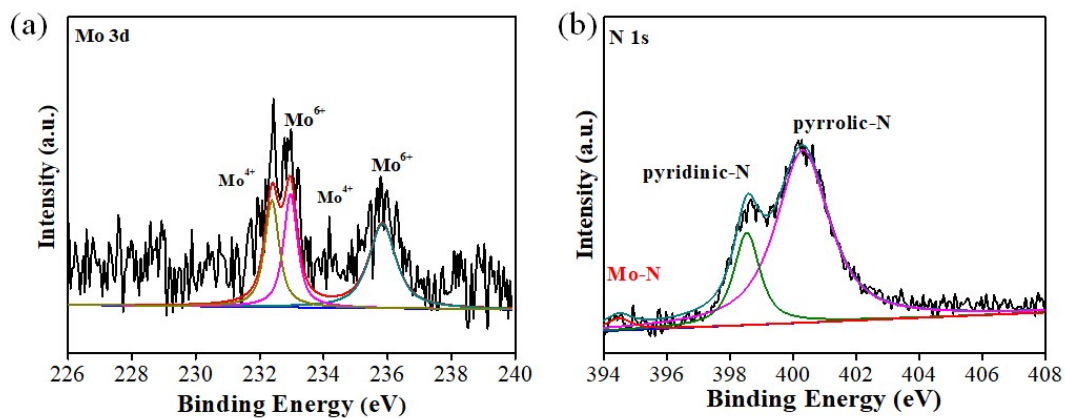


**Fig. S13.** (a) High-resolution Mo 3d XPS spectra and (b) high-resolution N 1s XPS spectra of Mo-N<sub>x</sub>/NPC@500.

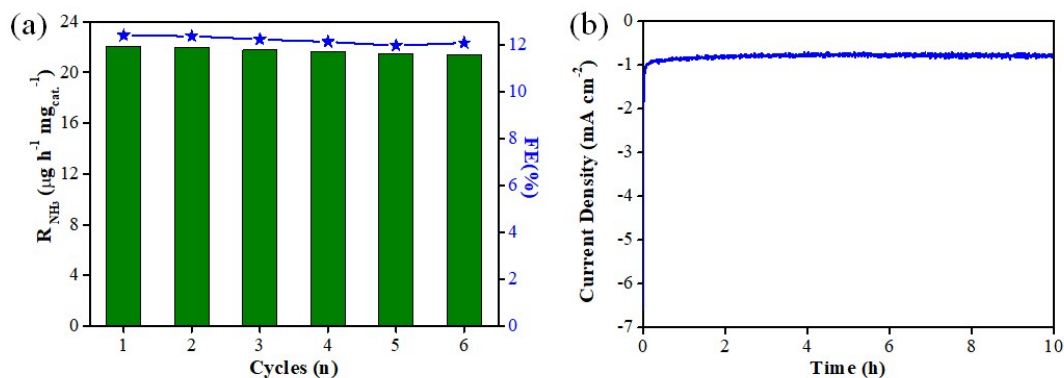


**Fig. S14.** (a) Stability test of Mo-N<sub>x</sub>/NPC@500 during recycling tests at  $-0.4$  V (vs.RHE) in N<sub>2</sub>-saturated 0.1 M Na<sub>2</sub>SO<sub>4</sub> electrolyte. (b) Time-dependent current density curve of Mo-N<sub>x</sub>/NPC@500 at  $-0.4$  V (vs.RHE) for 10 h in N<sub>2</sub>-saturated 0.1 M Na<sub>2</sub>SO<sub>4</sub> electrolyte.

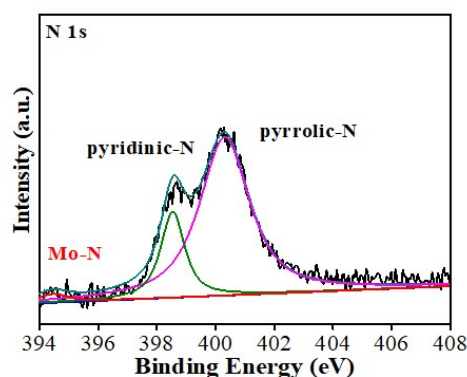


**Fig. S15.** High-resolution N 1s XPS spectra of Mo-N<sub>x</sub>/NPC@500 after long-term electrocatalysis at  $-0.4$  V (vs.RHE) in N<sub>2</sub>-saturated 0.1 M Na<sub>2</sub>SO<sub>4</sub> electrolyte.

## References

- 1 Y. Y. Liu, M. M. Han, Q. Z. Xiong, S. B. Zhang, C. J. Zhao, W. B. Gong, G. Z. Wang, H. M. Zhang, and H. J. Zhao, Dramatically enhanced ambient ammonia electrosynthesis Performance by in-operando created Li-S interactions on MoS<sub>2</sub> electrocatalys, *Adv. Energy Mater.*, 2019, **9**, 1803935.
- 2 S. Zhang, M. Jin, T. Shi, M. Han, Q. Sun, Y. Lin, Z. Ding, L. R. Zheng, G. Wang, Y. Zhang, H. Zhang, and H. Zhao, Electrocatalytically active Fe-(O-C)<sub>2</sub> single-atom sites for efficient reduction of nitrogen to ammonia, *Angew Chem. Int. Ed.*, 2020, **59**, 13423-13429.
- 3 S. Zhang, Q. Jiang, T. Shi, Q. Sun, Y. Ye, Y. Lin, L. R. Zheng, G. Wang, C. Liang, H. Zhang, and H. Zhao, ZIF-67-derived cobalt/nitrogen-doped carbon composites for efficient electrocatalytic N<sub>2</sub> reduction, *ACS Appl. Energy Mater.*, 2020, **3**, 6079-6086.